

APPLICATION OF THE ACOUSTIC EMISSION ANALYSIS TO HIGHLY THERMALLY LOADED COMBUSTOR SHIELDING PLATES

F. Meinel
Institut für Thermische Turbomaschinen
University of Karlsruhe (TH), Kaiserstrasse 12, 76131 Karlsruhe
Germany

ABSTRACT

Modern combustor shielding plates often show cracks due to high thermal loads. To prevent accidents, these shielding plates have to be investigated and changed frequently. Until today it is not clear, when these cracks develop and become a safety risk. With a better understanding of the crack propagation a higher durability and a cost effective application of these shieldings can be achieved. Thus the aim of this work was to investigate, whether the Acoustic Emission Analysis is able to detect thermal induced crack propagation during operation and monitor growing cracks or not. For these experiments a low-cycle fatigue test rig (LCF) was built up at the "Institut für Thermische Strömungsmaschinen" at the University of Karlsruhe. This test rig is able to simulate temperature gradients as they occur in real aircraft engines. The experiments have shown that the Acoustic Emission Analysis is able to detect and monitor thermal induced crack propagation. Two phases of different Acoustic Emission activity have been found. Further experiments showed, that the signals of the two phases vary significantly. It seems that these two phases with the different signal characteristics align with the first two stages of a fatigue crack: micro crack initiation and stable macro crack propagation. As a result the Acoustic Emission Analysis can be a helpful instrument for a better understanding and research of growing cracks under rough conditions.

1. BASICS

The Acoustic Testing, in short AT, is part of the non-destructive material test methods and is well known in seismology, pressure tank testing and materials science. Acoustic Emission, in short AE, is a process in the inner of a medium leading to an emission of acoustic waves. These acoustic waves spread out through a body and can be detected by adequate sensors and electronically evaluated. This application is called Acoustic Testing (AT). The typical frequency range in metals reaches from 50 kHz to several MHz.

Unlike other non-destructive methods, like X-ray, eddy current or ultrasonic testing, the Acoustic Testing is integral and completely passive and can be applied in-situ. With only a few sensors, large components can be tested and surveyed. However, the component must be loaded in such a manner that acoustic noise is emitted. Without inner changing of the material no noise is emitted and therefore the Acoustic Testing is not able to make any inference on the component. Only if the load exceeds a given minimum, Acoustic Emission Sources (AE-Sources), for example growing cracks, become active.

That means the AT is not able to measure the actual state but the deterioration of state.

In the following the most common terms of the AT as per guideline DIN EN 1330-9 (2000) [3] are elucidated:

1. Acoustic Testing (AT): Test method, based on Acoustic Emission.
2. Acoustic Emission (AE): Term for transient, elastic waves, resulting from release of (elastic stored) energy.
3. AE-event: Physical event producing AE, e.g. crack formation
4. AE-source: Physical source of one or more AE-events. This can be crack growing step by step. Each growing of the crack is an AE event.
5. AE-signal: The electrical signal of the sensor resulting from AE.
6. Transient signal, burst: AE-signal with clearly detectable start and end.
7. Hit: Burst detected by the AE-system.
8. AE-activity: Occurrence of AE-signals as a result of AE.

1.1. Acoustic Emission-parameters

Due to the very high frequency measured in metal structures (up to several MHz) the sampling rate of the AE-system must be very high too (usually 10 MHz). This high sampling rate together with a bit depth of 16 bit leads to an enormous need of disc space. In order to reduce disc space, not the complete time signal is saved. Only the parts with AE-signals and a certain number of AE-parameters are saved. FIG 1 shows the parameters of an AE-signal.

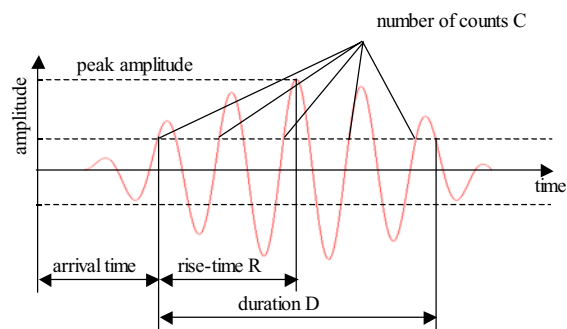


FIG 1: Acoustic Emission-parameters

To start the storage and the calculation of the parameters, a given threshold has to be exceeded. The time of the first threshold crossing, either positive or negative, is called "arrival time of the burst" and is needed for the location

calculation. A transient AE-Signal ends, when there are no more threshold crossings after a fixed time span. The time between the first and the last threshold crossing is called duration D [μs]. Other parameters are "arrival time" t_a (time to the first crossing) [μs], rise-time R (time from t_a to peak amplitude) [μs], number of threshold crossings (Counts) C [-], peak amplitude A_{max} [dB^1 , mV] and the energy E [Eu] of an AE-signal. Eu is per definition the squared signal, integrated over the time [5], the unit is V^2s . All parameters are dependent on the threshold, hence measurements with different thresholds are hardly comparable.

1.2. Location of an Acoustic Emission-source

In the Acoustic Testing, the location of AE-sources, for example growing cracks, is an essential element. The location calculation is based upon time offsets between the arrival times for spread sensors. The time offsets are proportional to differences in distance, see equation (1).

$$(1) \Delta t = \Delta s/c$$

For this calculation, the speed of the propagating waveform is needed. Structure borne noise is not bound to only one waveform (like air borne noise), there are a lot of different waveforms. For a proper result, the dominant propagating waveform and its speed has to be known.

The calculated distances can be converted into the coordinates of the AE-source. For this conversion on a 2-D object, a minimum of three sensors is necessary. For a proper location calculation, the AE-source must be in the area in between the sensors.

2. EXPERIMENTAL SETUP

The following sections describe the test carrier and the test rig in which the combustor shielding plate can be thermo-cycled.

2.1. Acoustic Emission-analyzer

For the AE-experiments the "AMSY-4" analyzer (Vallen Systeme GmbH, Munich) was used. It was equipped with four AE input channels with sampling rate of 10 MHz and a bit depth of 16 bit. Each channel is equipped with two analogue high-pass filters (25 kHz and 230 kHz) and one analogue low-pass filter (5 MHz). Furthermore each channel has a parameter extraction and a transient wave recorder. In addition the "AMSY-4" was provided with four parametric inputs to record external voltage signals, like temperature or pressure measurement signals. That makes it easy to associate changing AE-activity with changes in pressure or temperature. Through the inputs the external pre-amps can be supplied with a 28 V_{DC} phantom power. These pre-amps amplify the weak signal from the sensors, so that it can be sent over a greater distance.

2.2. Acoustic Emission Sensors

In the Acoustic Testing, piezo-ceramic sensors have established. There are two types of sensors: broadband

sensors and resonant sensors. The latter have a resonance in their measurement range and therefore a far higher sensitivity. This resonance frequency and its bandwidth can be adapted to the application. Broadband sensors have a linear sensitivity over their frequency range, but are less sensible than the resonant ones. The electrical signal is not necessarily identical with the original mechanical impulse. For example Eigen frequencies or sensor characteristics can influence the electrical signal. High sensible resonant sensors in particular have a great influence on the measured signal. The measured frequency spectra are virtually identical to the Eigen frequency spectra of the sensor.

The sensors used in this experiment were resonant type sensors "VS375-M" (Vallen Systeme GmbH, Munich), see FIG APP 1. To determine the background noise of the test rig, broadband sensors "B-1025" (Digital Waves) have been used. Both sensors have a maximal working temperature of 100 $^{\circ}\text{C}$.

2.3. Low Cycle Fatigue Test rig

The Low Cycle Fatigue (LCF) rig consists of a gas fired burning chamber, whose input air can be preheated up to 1123 K at 10 bars. This preheated air is also used for the cooling of the shielding plate. The exhaust gases of the burning chamber have a temperature up to 2000 K, depending on the amount of gas. The hot exhaust gases run over the shielding plate, which is cooled with the preheated air.

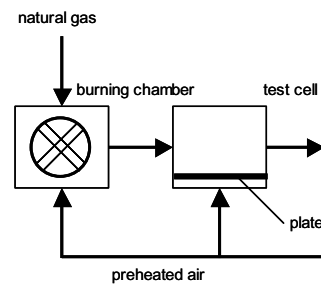


FIG 2: Low Cycle Fatigue test rig

The thermal cycles are controlled by an automatic control system that adjusts the mass flow of the gas and the pressure in the LCF rig. So repeatable cycles can be run. A single cycle can be divided in the following sections: idle, heating, full load, cool down, as shown in FIG 3.

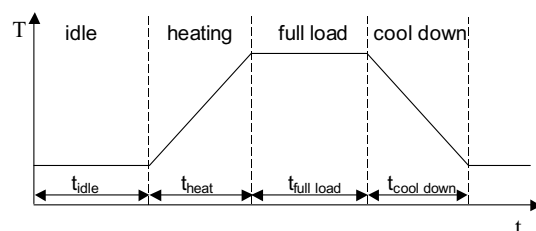


FIG 3: Thermal cycles

The idle and full load times were set to 30 seconds each, the heating time was 17 seconds and the cool down 22 seconds. The idle temperature was 900 K, the full load temperature 1400 K and the pressure was 7,7 to 8,5 bars.

¹ $A[\text{dB}] = 20 \cdot \log(U/U_{\text{ref}})$ with $U_{\text{ref}} = 1 \mu\text{V}$

2.4. Test carrier

FIG 4 shows a principal drawing of the shielding plate, assembled on the carrying plate. The shielding plate is screwed on the carrying plate. The arrows mark the directions of mass flow. The preheated air flows through holes in the carrying plate, on the one hand feeding the film slot and on the other hand, feeding the effusion cooling of the plate.

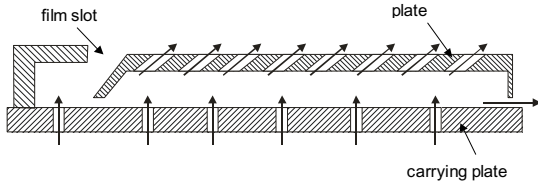


FIG 4: Principal drawing

FIG 5 shows the section and the top view of the tested shielding plate. The plate is made of chrome-nickel steel X5CrNi18-10 (No. 1.4301) and has a thickness of 2 mm. The plate carries 63 holes with a diameter of 0,9 mm and 34 holes with a diameter of 1,2 mm, all under an angle of 30°. The surface temperature is measured with a thermocouple (Type K), caulked on the hot air surface of the plate.

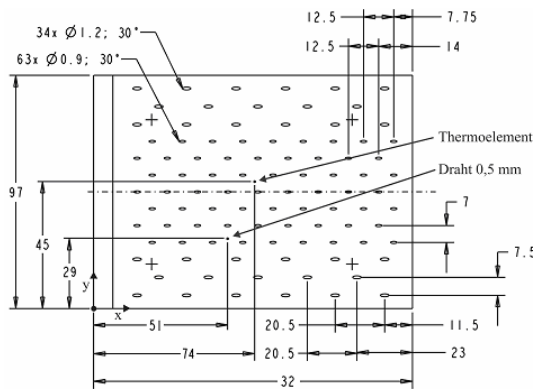


FIG 5: Geometry of the shielding plate

Due to the high temperatures on the plate (up to 1000 K) and the maximum working temperatures of the sensors (373 K), they could not directly be placed on the plate. The acoustic waves had to be routed out into cooler conditions. For this purpose four waveguides had been welded on the plate and led out of the test rig, where the sensors have been connected to the waveguides, see FIG 6.

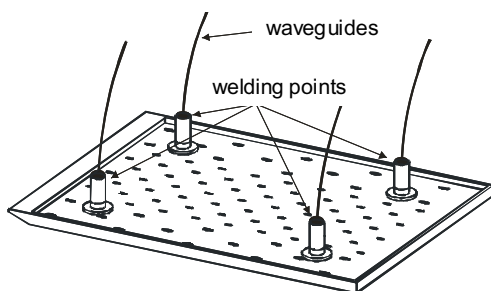


FIG 6: Waveguides on the plate

For a good sound transition from the plate into the waveguides, they are made of the same material as the plate. The waveguides have a thickness of 2 mm with a length of 520 mm, see FIG 6.

3. PRELIMINARY EXPERIMENTS

3.1. Reduction of disturbance sources

Because of the low level of energy emitted during crack propagation, even marginal perturbation can have great influence on the measurement. Therefore, the elimination of disturbance sources is a crucial factor. The aim was to achieve as much structure borne sound isolation as possible. One point was to reduce the sound transition through the screwing points of the shielding plate. To achieve that, all screws, bolts and nuts have been provided with carbon washers. Carbon has a well different acoustic impedance than steel, meaning a bad sound transition. Furthermore carbon has a very little coefficient of friction. This means a higher mobility and less emitted friction noise. The other point was the sound isolation at the sealings of the waveguides. The sealings were made of Teflon, providing a well different impedance as well.

In the following experiments the effectiveness of the actions was tested. With both actions a minimum structure borne sound isolation of 52 dB has been achieved.

In order to gain a high signal to noise ratio (SNR), the background noise of the running LCF-rig was measured. Three broadband sensors were placed on the rig and one was used as reference on a vibration isolated steel bar. The highest detected peaks had about 75 dB. With a maximum working range of 100 dB of the AT-equipment, the SNR is only 25 dB. With such a little SNR transient AE-signals with low energy and amplitude can not be differentiated from the background noise. A possibility to gain a better SNR is the use of frequency filters. For this purpose the frequency spectra of a normal crack signal and the background noise have been analysed. FIG 7 shows the frequency spectrum of the measured background noise.

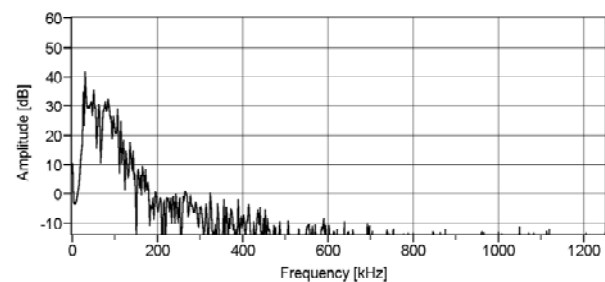


FIG 7: Spectrum of the background noise

The strong characteristic below 200 kHz is clearly visible. In comparison FIG 8 shows the spectra of a normal crack signal with broadband characteristic. In order to achieve a better SNR, the electrical signals can be filtered, for example with a 200 kHz high-pass filter. As FIG 8 shows, the filtering should have little or no negative effects on the detectability of the signals.

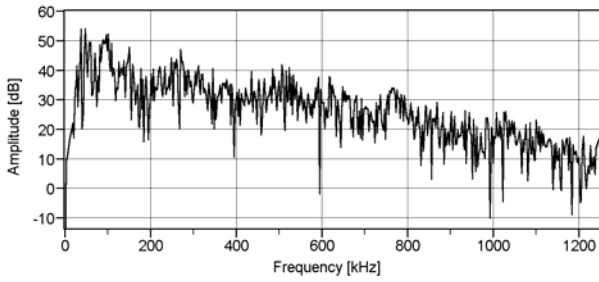


FIG 8: Spectrum of a crack signal

The cut-off frequency of the (analogue) high-pass filter was set to 230 kHz with a slope of 54 dB/octave. Furthermore the resonance frequency of the sensors was chosen to 375 kHz. This reduces the influence of low frequencies even more. These two actions have reduced the influence of the background noise to a level less than 28 dB. Only these application and the use of carbon washers and Teflon sealings have made a measurement of AE-signals possible.

3.2. Location calculation

For a proper localisation calculation the speed of the dominant propagating wave form is needed. In solid bodies several wave forms can exist. They can be distinguished in volume and surface waves. Because of the plate's thickness of only 2 mm, volume waves can not develop. Hence the expected wave forms are surface waves, here Rayleigh- and Lamb-waves. Lamb waves are basically two interfering Rayleigh-waves on the opposite surfaces of a thin plate. These two waves can be symmetrical (s-modes; mirrored along the plates middle) or anti-symmetrical (a-modes; mirrored plus 180° out of phase). Theoretically an infinite number of modes can develop on such a plate, but their number is limited with regard to a given frequency [7].

FIG 9 shows the calculated dispersion curves of the phase velocities on a 2 mm thick plate made of X5CrNi18-10. The frequency range of interest here is below 0,5 MHz. There are three possible waveforms in this frequency range: the s_0 -Lamb mode, the a_0 -Lamb mode and the Rayleigh wave. Due to the higher velocity of the s_0 -mode, this mode is expected to be the crucial wave form.

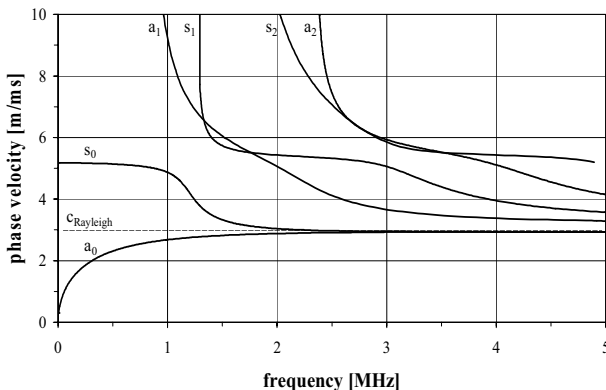


FIG 9: Phase velocities of Lamb waves

For the subsequent AE-experiments, it is important to know how the speed of the wave form reacts to changes in temperature. For this reason, several tests have been performed. Through an additional (fifth) waveguide test signals have been sent into the plate. The sensors detect the signal and the analyser calculates the position of the sound entry (welding point of the fifth waveguide). These tests have been carried out for various temperatures. For a correctly assumed speed of sound, the calculated source of sound must be equal to the real source. The more the assumed speed of sound differs from the real one, the more the calculated and the real source of sound differ. The difference between the real and calculated position is called location uncertainty.

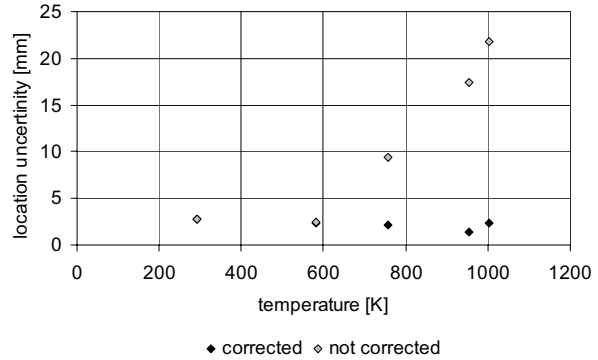


FIG 10: Influence of the temperature on the location uncertainty

FIG 10 shows the influence of temperature on location uncertainty. If the location calculation (that means the assumed speed of sound) is not adapted to the temperature, the location uncertainty can become very large. With an adaptation, the uncertainty stays below 2,7 mm. This means, all calculated sources lie within a circle with a radius of 2,7 mm around the real source.

4. RESULTS AND DISCUSSION

In the following sections the results of the AE-experiments are presented and discussed. First of all it has to be mentioned, that the shielding plate didn't show any damage after the thermo cyclic tests. Even by an inspection with a microscope no cracks have been detected. However during the AE-experiments a high AE-activity occurred, that respective source apparently did not lie on the plate. Therefore the reason of that AE-activity has to be identified. Subsequently an overview over the test procedure and the measured data will be given. Finally the results of the AE-experiments will be discussed in detail.

4.1. Reason for the Acoustic Emission-activity

The signals measured during the thermo cyclic tests have clearly transient character. This excludes reasons like leakage or friction, which generate continuous signals. The signal in FIG 11 has a clear beginning and a fast rising amplitude, which is typical for crack signals.

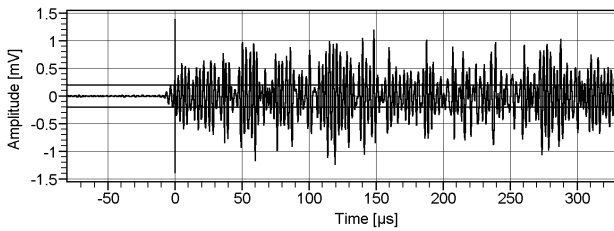


FIG 11: Transient crack signal

However, it was not possible to calculate the sources of these AE-signals. As mentioned above, a location calculation is only possible if the source is in the area in between the sensors. This allows the assumption that the signals do not have their source on the shielding plate. By checking the so called “first hit-sensors”, the direction of sound can be determined. A “first hit-sensor” is the sensor, which is the closest to the AE-source and therefore detects the signal at first. The two sensors with the first hits are the sensors at the upstream edge of the plate, right next to the film cooling outlet.

Taking these two facts into account, it seems that the AE-sources lie upstream, outside of the plate. This was verified by the demounting of the test carrier after the experiments. The weld seams of the carrying plate and the film cooling, lying upstream of the plate, showed big cracks.

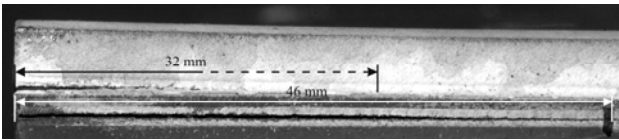


FIG 12: Carrying plate, detail left crack

These cracks definitely developed during the AE-experiments. The total length of the cracks on the carrying plate is 101 mm (left crack 71 mm, right crack 30 mm) and on the film cooler 32 mm.

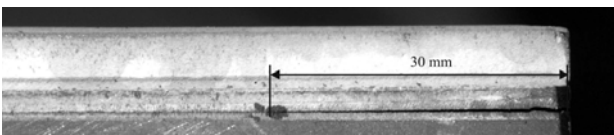


FIG 13: Carrying plate, detail right crack

Finally it is not clear, which channel the sound did take into the plate or the waveguides. It might have bridged over the carbon washers into the bolts.

4.2. Thermo cycles

FIG APP 2 shows the measured data over the total test time. It shows the run of the total pressure, hot air, cooling air and the plate’s surface temperature and the hot air mass flow. A number of 96 cycles have been run. These cycles can be divided into four blocks. In the first block (start: 1265 s, end: 6300 s) the control parameters for the automatic control have been adjusted. For this reason these cycles are not identical. At 6330 s the second block begins. Because of a test rigs dysfunction it ends at 9600

s (33 cycles). The third block starts at 9900 s and ends due to another dysfunction at 13600 s (34 cycles). Block four is the last block, starting at 14800 s and ending at 15000s. With block four the AE-experiments end. Excluding block one, a total number of 70 identical cycles has been run. The following table gives an overview over the relevant test data.

absolute total pressure:	≈ 7,7 bar – 8,5 bar
absolute static pressure:	≈ 7,7 bar – 8,5 bar
mass flow hot air:	400 g/s – 700 g/s
mass flow cooling air:	~ 5 g/s – 25 g/s
temperature hot air:	600 K – 1500 K
temperature cooling air:	480 K – 575 K
surface temperature plate:	500 K – 1000 K
blowing rate film cooling:	0,25
blowing rate effusion cooling:	3,1

TAB 1: Measurement data

In FIG APP 3 two cycles are shown in detail. For the thermo-cyclic strain, the temperature gradients on the shielding plate are a matter of particular interest. The average temperature gradient for the heating period is about 25 K/s for the hot gas and 6 K/s for the plate. For the cool down period the temperature gradients are about –11,3 K/s for the hot gas and –5,3 K/s for the plate. The absolute maxima of the temperature gradients are 77 K/s and –31 K/s for the hot gas and 15 K/s and –12 K/s for the plate’s temperature. The temperatures and therefore the temperature gradients in the broken weld seams are not known, but are assumed to be alike the temperatures on the plate.

4.3. Results of the Acoustic Emission-experiments

In the following sections the results of the AE-experiments are discussed. It will be clarified, whether the measured Acoustic Emission can be associated with the stages of crack propagation. First the progress of the AE will be discussed over the whole testing time. It will be investigated, if phases of different AE-activity occurred. Then will be investigated, if the AE-signals can be sorted into different classes. The last point will be to check if the found classes align with the found phases.

4.3.1. Acoustic Emission-activity over the hole testing time

FIG APP 4 gives an overview over the peak amplitudes of the measured AE-signals. Every dot marks a measured AE-signal for a given sensor. There are no signals measured below 46.1 dB due the threshold. The profiles of the hot gases and the shielding plate’s temperature are plotted as well. Disturbing signals coming from friction or leakage can be excluded; they would appear all over the time. The first AE-activity occurs at 4200 s. In this block the control parameters for the automatic control system have been adjusted. The abrupt beginning of the AE-activity at 4200 s is likely to be led back to an increase of the hot gas temperature and a decrease of the cooling air temperature. This leads to higher temperature gradients in the plate and thus to a higher strain. The increase of strain was probably that high, that the weld seals started to emit sound. The level of the pre damage of the weld

seals is not known. Therefore it can not be distinguished if this emission is the very first or a continued emission from earlier experiments.

The signals in the first and second block occur sporadically and have a strong amplitude dispersion. At the end of the second block the signals start to accumulate. In the third block the amplitude dispersion gets smaller. The rate of the AE-events seems to stay constant, with slightly increasing amplitudes. This proceeds in the fourth block. The signals at the very end of the measurement (after block four) occurred during the switch off of the test rig. These signals have been measured during the pressure release. The temperature of the shielding plate had already decreased below 500 K. So these signals cannot be associated with thermally induced crack propagation. They seem to be disturbing signals due to the pressure release, for example loosening of restraints. Thus, two phases of different AE-activity can be distinguished: a first phase with sporadic activity and a high amplitude dispersion and a second phase with a high number of AE-events with less amplitude dispersion.

For the evaluation of Acoustic Emission it can be reasonable, to have a closer view on the rate of the AE-events. The AE-rate is the number of AE-events per time unit. With a summation of all AE-events over the time, changes in the AE-rate can easily be detected. For example a time period with constant AE-rate becomes a straight line. Changes in the AE-rate can have manifold causes. For example a rising load can increase the AE-rate or the crossover from stable to instable crack propagation. FIG APP 5 shows the curve of the accumulated AE-events. Expectedly, the curve is very flat far into the second block (see phase I). During that time only little AE-activity did occur. From 9000 s the AE-rate starts to rise until it reaches a steady state AE-rate at 11100 s (see phase II). Block four shows the same gradient. Thus, the accumulation of the AE-events confirms the two phases found in the amplitudes. Furthermore it can be seen that the cumulated curve has a step character. This phenomenon will be discussed later. The peak energy of the AE-events and the accumulated energy (not shown in this paper) have the same characteristics.

As FIG APP 5 shows, the measured Acoustic Emission can be distinguished in two phases. On the basis of the first two stages of a fatigue crack, micro crack initiation and macro crack propagation [2], the two phases found in this paper can be classified correspondingly. At the end of the durability of a material it comes the third phase of a fatigue crack, the unstable fracture. As FIG 12 and FIG 13 show, an unstable crack propagation did not occur. Also the AE-signals do not show the beginning of unstable crack propagation. This would cause a rapidly rising energy and AE-rate because of the fast growing crack. The cracks in the weld seals have therefore been in the second phase of a fatigue crack: the stable crack propagation.

4.3.2. Classifying of the Acoustic Emission-signals

In this section is discussed, whether the above introduced phases of different AE-activity do vary in their signal

characteristics as well. Crack initiation and crack growing do vary physically, for example in consumed energy, developed crack length, etc. Therefore it seems that the emitted signals differ as well. In this case, typical signals according to the phases should be found. This type differentiation happens by plotting two AE-parameters against each other, for example counts against amplitude. In the ideal case several data accumulations arise that can be differed from each other and align with the phases. This is also a good instrument to identify disturbing signals.

FIG 14 shows the counts over the peak amplitude of the measured signals.

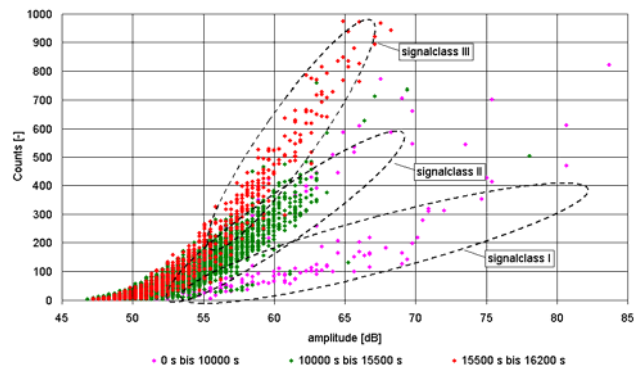


FIG 14: Signal classes

Three classes can be identified. To check whether these classes correspond with the phases found in FIG APP 5, the measured signals have been coloured according to time intervals. These time intervals correspond with the phases found in FIG APP 5. It can be seen clearly, that the phases have significantly different signal character. The signals in the “signalclass I” belong to the phase I, the micro crack initiation. The signals in the “signalclass II” belong to the phase II, the stable macro crack propagation. The signals in the “signalclass III” have their source in the pressure release of the test rig. Because of the fact, that the signals during the pressure release form a separate class, it is very likely that these signals are disturbing and not crack signals. Further systematic disturbing signals would form yet another class. But as FIG 14 shows, no other classes can be found. Therefore, it can be assumed that during the measurement only a few disturbing signals occurred.

In [6] AE-experiments signal classes have been found as well that did correspond with the phases of damage. In [6] classes for the phases “creation of lueders bands”, “micro crack initiation”, “creation of major cracks” and “propagation of macro cracks” have been found. It was shown, that only a few signals with highly dispersing characteristics appeared during “creation of lueders bands” and “micro crack initiation”. The major part of the signals was found in the phase “propagation of macro cracks”. In the present experiments also two phases have been found: one phase with little activity and dispersing characters and another phase with the major part of the AE-activity. Therefore the “signalclass I” stands for the micro crack initiation and the “signalclass II” for the stable macro crack propagation, see FIG 15.

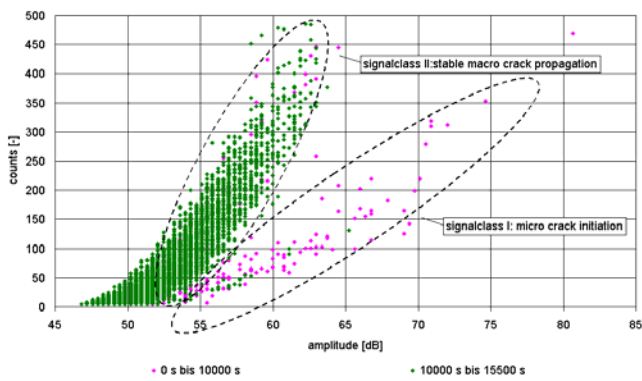


FIG 15: Signal classes 2

4.3.3. Acoustic Emission-activity in a single cycle

This section clarifies, whether the Acoustic Emission corresponds with the sections of the thermal cycles. As FIG 16 shows, virtually all AE-events occur during the cool down phase, in fact in the areas of the highest negative temperature gradients.

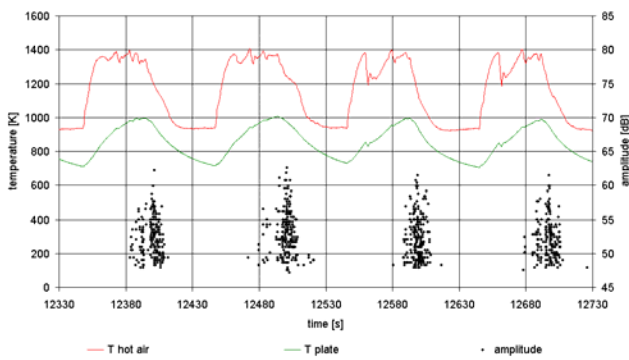


FIG 16: Amplitudes during stable macro crack propagation

FIG 17 shows the same: the changes in the AE-rate occur in the cool down phase, resulting in the step character of the AE-activity.

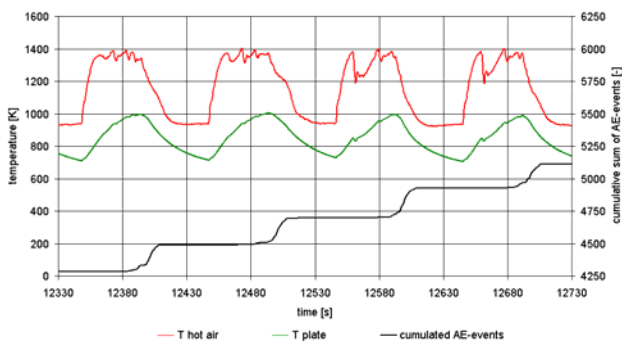


FIG 17: Cumulative hits during stable macro crack propagation

Finally it is discussed which mechanisms lead to the crack propagation and therefore to AE-activity during the cool down phase. [4] and [1] show that thermal fatigue is based on inner and outer force. Inner forces result from temperature gradients inside of the material. The hot gases side of the shielding plate has a higher temperature than the cooled side. These temperature gradients lead to thermally induced tensions. As per [1], this leads to permanent tensions on the cooler surface.

The outer forces are induced due to a hindrance of thermal elongations, for example due to fixed supports. In the heating phase compression stresses occur, whereas tensile stresses occur during the cool down [4]. During the cool down phase the tensions induced by inner and outer force do overlay. These tensions lead to an overstraining of the weld seals and therefore to crack propagation.

However the cracks did occur in the weld seals of the carrying plate, the results and conclusions drawn in this paper can be transfused onto the shielding plate. The tensions overlays as well on the shielding plate and can lead to crack propagation. The classification of the AE-signals seems also possible for cracks on the shielding plate. Additionally, the location of the AE-sources can give a better insight into the crack propagation. The reason for no crack propagation on the plate is a too small thermo cyclic load in the test rig. With a new, more durable, carrying plate, the thermal loads can be increased, leading to crack propagation on the shielding plate.

5. CONCLUSION

The aim of this work was to investigate, whether the Acoustic Testing is able to detect thermal induced crack propagation during operation. For these purposes an adequate shielding plate with waveguides was designed. Furthermore, sound isolation actions and a filtering of the electric signals have been used in order to reduce disturbances. For a proper location calculation the speed of sound for various temperatures has been determined. It was shown, that the speed of sound should be adapted to the actual surface temperature of the shielding plate.

During the thermo cyclic tests the shielding plate did not show any crack propagation. The measured Acoustic Emission signals came from cracks in the weld seals of the carrying plate that developed during the thermo cyclic tests. These signals have been divided into two phases of different Acoustic Emission activity. Furthermore the signals have been classified into several, independent signal classes. These classes did match with the phases of different Acoustic Emission activity. These phases align with the first two phases of a fatigue crack: micro crack initiation and stable macro crack propagation. In this paper it was proven, that the Acoustic Emission Analysis is able to detect crack propagation online and under rough conditions. Above that it was shown that the crack signals itself can give information about the progress of damage.

6. LITERATURE

- [1] David, P. (2006): Beschreibung relevanter Hochtemperaturschädigungsmechanismen und messtechnischer Verfahren zum Rissnachweis in Brennkammerschindeln; diplomathesis, Institut für Thermische Strömungsmaschinen; Universität Karlsruhe (TH)
- [2] Bargel, H.-J., Schulze, G. (2000): Werkstoffkunde; Springer Verlag Heidelberg
- [3] DIN EN 1330-9 (2000): Materialprüfnormen für metallische Werkstoffe 2; DIN-Taschenbuch 56; 6. Auflage; Beuth-Verlag Berlin
- [4] Hollerich, T. (2006): Grundlegende, experimentelle Untersuchungen zum schwingungsbasierten Rissnachweis in Brennkammerschindeln; diploma thesis, Institut für Thermische Strömungsmaschinen; Universität Karlsruhe (TH)
- [5] N.N. (2002): Schallemissionsprüfung – Grundlagen, Gerätetechnik, Anwendungen; Vallen – Systeme GmbH; D – 82057 Icking (München)
- [6] Timmers, R. (2002): Schallemissionsuntersuchungen bei LCF-Versuchen an Baustahl ST-45; dissertation at the Universität Dortmund
- [7] Viktorov, A. (1967): Rayleigh and Lamb Waves; Acoustic Institute; Academy of Sciences of the USSR; Translation by Warren Manson, Columbia University

7. APPENDIX

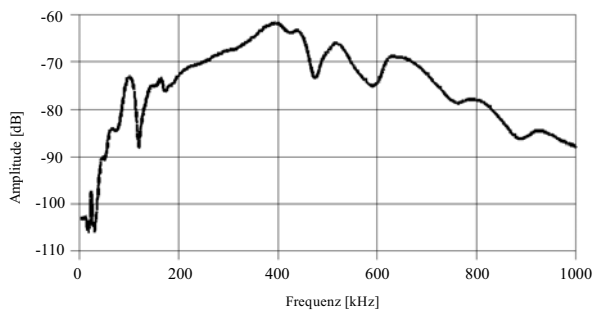


FIG APP 1: Spectra of „VS375-M“

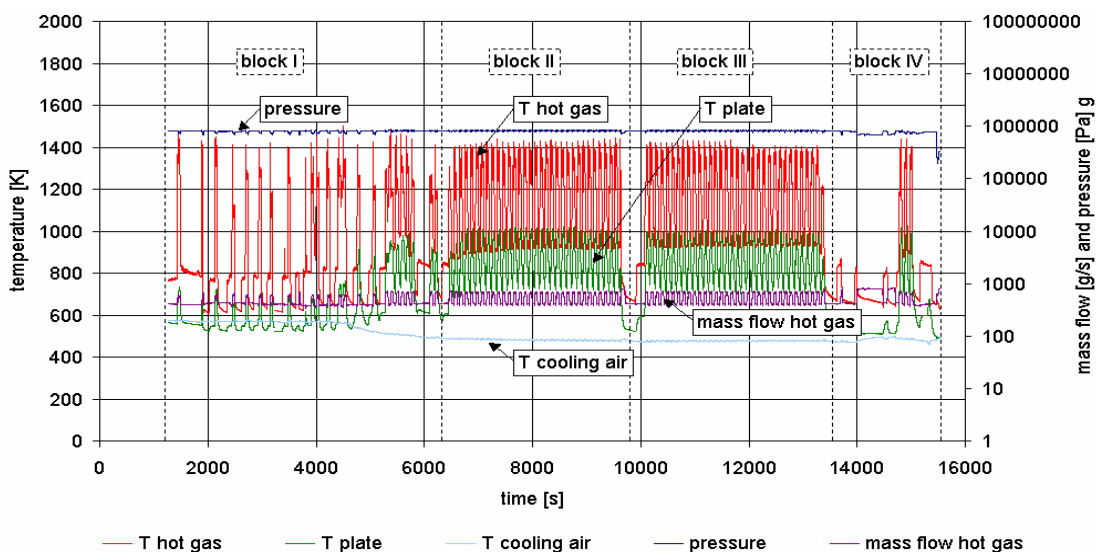


FIG APP 2: Measured data during the thermal cycles

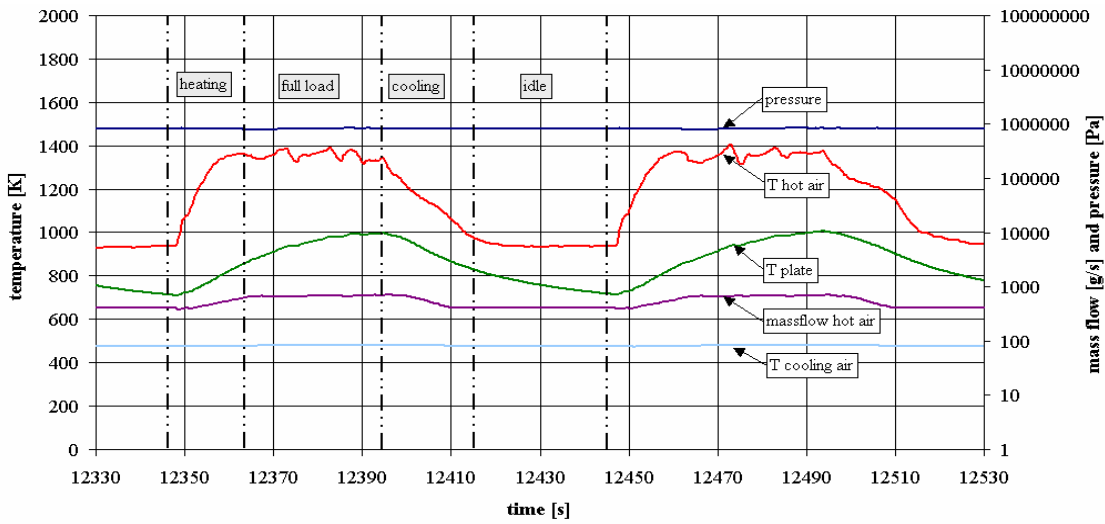


FIG APP 3: Measured data for two cycles

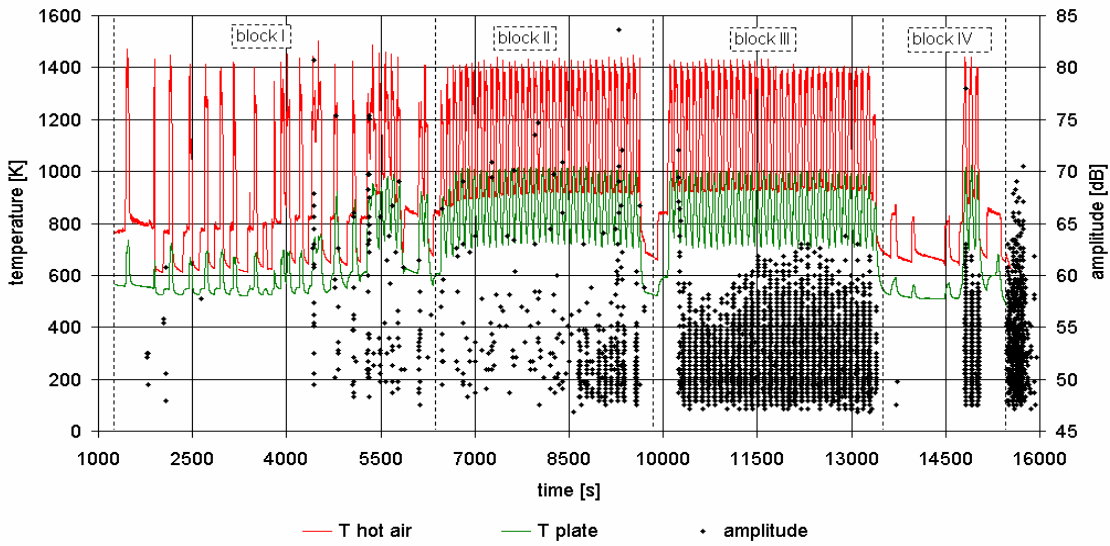


FIG APP 4: Peak amplitudes of the measured AE-signals

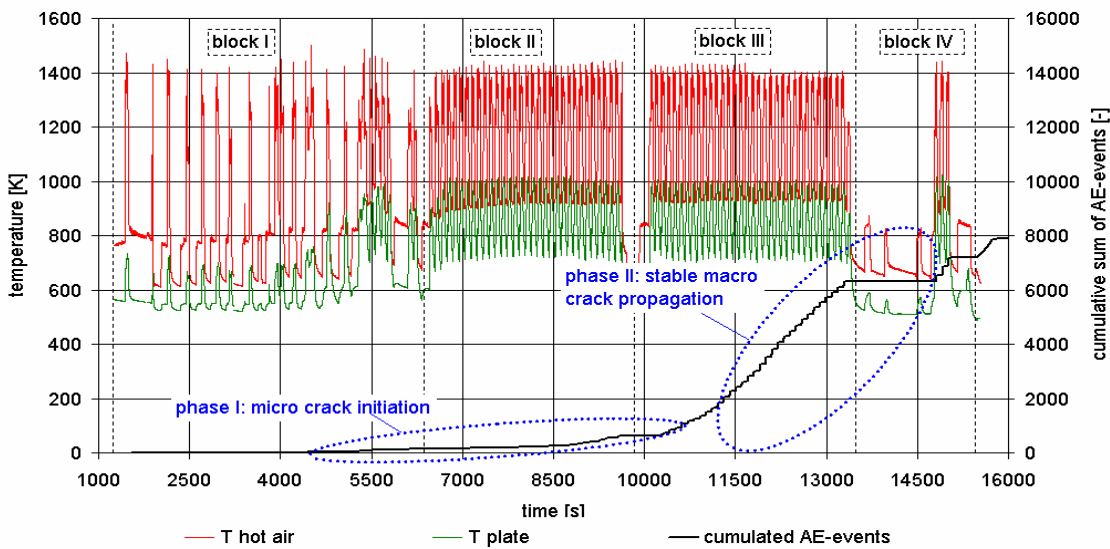


FIG APP 5: Summation of AE-events